Biosci. Rep. (2008) / **28** / 83–88 (Printed in Great Britain) / doi 10.1042/BSR20080002

Original Paper

Bioscience Reports

Stimulation of mitochondrial proton conductance by hydroxynonenal requires a high membrane potential

Nadeene PARKER*[1], Antonio VIDAL-PUIG† and Martin D. BRAND*

*MRC Dunn Human Nutrition Unit, Wellcome Trust/MRC Building, Hills Road, Cambridge CB2 0XY, U.K., and †Metabolic Research Laboratories, Level 4, Institute of Metabolic Science, Box 289, Addenbrooke's Hospital, Cambridge CB2 0QQ, U.K.

Synopsis

Mild uncoupling of oxidative phosphorylation, caused by a leak of protons back into the matrix, limits mitochondrial production of ROS (reactive oxygen species). This proton leak can be induced by the lipid peroxidation products of ROS, such as HNE (4-hydroxynonenal). HNE activates uncoupling proteins (UCP1, UCP2 and UCP3) and ANT (adenine nucleotide translocase), thereby providing a negative feedback loop. The mechanism of activation and the conditions necessary to induce uncoupling by HNE are unclear. We have found that activation of proton leak by HNE in rat and mouse skeletal muscle mitochondria is dependent on incubation with respiratory substrate. In the presence of HNE, mitochondria energized with succinate became progressively more leaky to protons over time compared with mitochondria in the absence of either HNE or succinate. Energized mitochondria must attain a high membrane potential to allow HNE to activate uncoupling: a drop of 10–20 mV from the resting value is sufficient to blunt induction of proton leak by HNE. Uncoupling occurs through UCP3 (11%), ANT (64%) and other pathways (25%). Our findings have shown that exogenous HNE only activates uncoupling at high membrane potential. These results suggest that both endogenous HNE production and high membrane potential are required before mild uncoupling will be triggered to attenuate mitochondrial ROS production.

Key words: adenine nucleotide translocase (ANT), 4-hydroxynonenal (HNE), mitochondria, proton leak, uncoupling protein 3 (UCP3)

INTRODUCTION

Mitochondria are the major producers of intracellular ROS (reactive oxygen species) [1]. Oxidative stress and mitochondrial dysfunction caused by the overproduction of ROS have been implicated in several degenerative diseases and are also thought to be a major contributor towards the ageing process [2].

The mild uncoupling of electron transport from ATP production in mitochondria has been shown to severely blunt their production of ROS [3,4]. This uncoupling can be achieved via the leak of extruded protons back into the mitochondrial matrix through pathways other than ATP synthase. Suggestions have been made that ROS themselves, possibly via downstream lipid peroxidation products, act in a negative feedback loop to attenuate their own production by inducing such a proton leak [4,5]. Peroxidation of membrane phospholipids by ROS leads to a self-propagating chain of free radical reactions. These reactions culminate in the production of a largely cytotoxic mix of aldehydes, alkenals and hydroxyalkenals [6]. Of these ROS-derived lipid peroxidation products, HNE (4-hydroxynonenal) is known to be particularly reactive and is implicated as an important mediator of free-radical damage [6]. It has been shown that cytotoxic HNE is also able to act as a signalling molecule, inducing mitochondrial uncoupling via the mitochondrial carriers, specifically uncoupling proteins (UCP1, UCP2 and UCP3) and ANT (adenine nucleotide translocase) [7].

The mechanism of induction of proton leak by HNE is unclear [8]. It has been postulated that covalent modification by HNE causes conformational changes in the UCPs which allow the passage of protons back into the mitochondrial matrix [9]. HNE stimulation of proton leak is sometimes elusive, presumably because it is condition-dependent; Esteves et al. [10] clearly showed HNE-stimulated uncoupling via UCP1, whereas Shabalina et al.

Abbreviations used: ANT, adenine nucleotide translocase; HNE, 4-hydroxynonenal; KO, knockout; ROS, reactive oxygen species; TPMP, triphenylmethylphosphonium; UCP, uncoupling protein; WT, wild-type.

[1]To whom correspondence should be addressed (np@mrc-dunn.cam.ac.uk).

[11] did not. In the present study we have used skeletal muscle mitochondria isolated from rats and WT (wild-type) and *Ucp3*-KO (knockout) mice to clarify the conditions necessary to induce HNE-dependent uncoupling. We have also assessed the relative contributions of different HNE-associated uncoupling pathways.

EXPERIMENTAL

Animals

Female Wistar rats (Charles River), and male and female mice, were housed at $21 \pm 2^{\circ}C$ and $57 \pm 5\%$ humidity in a 12 h light/12 h dark cycle, with standard laboratory chow and water ad libitum, following U.K. Home Office Guidelines for the Care and Use of Laboratory Animals. *Ucp3*-KO [12] and WT sibling-paired mice were used at the age of 12–15 weeks. *Ucp3*-KO was confirmed by PCR analysis of genomic *Ucp3* and Western blotting of skeletal muscle mitochondria.

Mitochondria

Animals (1 rat or 4 mice per preparation) were killed by stunning and cervical dislocation. Mitochondria were isolated from total hind-limb skeletal muscle [13]. Mitochondria from WT and *Ucp3*-KO mice were prepared and assessed in parallel.

Proton leak kinetics

The rate of oxygen consumption required to pump the protons back out of the mitochondrial matrix (in the presence of oligomycin to prevent ATP synthesis) is directly proportional to the proton leak rate across the inner membrane of isolated mitochondria [14]. Proton leak kinetics were measured as the dependence of proton leak rate on its driving force, protonmotive force (measured as membrane potential in the presence of nigericin to abolish pH gradients). Membrane potential and respiration rate were measured simultaneously using electrodes sensitive to the membrane-potential-dependent probe TPMP (triphenylmethylphosphonium) or oxygen. The assay medium contained 0.35 mg/ml mitochondrial protein, 120 mM KCl, 5 mM KH_2PO_4, 3 mM Hepes, 1 mM EGTA, 0.3% (w/v) defatted BSA, 5 μM rotenone, 1 μg/ml oligomycin and 0.11 μM nigericin. The TPMP electrode was calibrated with sequential additions of 0.5 to 2.5 μM TPMP and the mitochondria were energized with 4 mM succinate. Leak kinetics were measured by varying membrane potential and oxygen consumption by sequential additions of malonate (approx. 0.1–2.3 mM). After each experiment, 0.2 μM FCCP (carbonyl cyanide *p*-trifluoromethoxyphenylhydrazone) was added to release matrix TPMP, allowing correction for any small baseline drift. The TPMP binding correction was taken to be 0.35 mg of protein/μl [15].

Statistics

Respiration rates (by linear interpolation between flanking points) at the highest membrane potential common to all conditions on a given day were used to test for differences in proton conductance by ANOVA or paired Student's *t* tests. The results are expressed as the means ± S.E.M. for each condition, with the mean value of the highest common potential indicated.

RESULTS

Energization-dependent increase in HNE-stimulated proton leak in rat skeletal muscle mitochondria

Skeletal muscle mitochondria, when energized with succinate, show a time-dependent uncoupling via an endogenous activation of UCP3, ANT and other uncoupling pathways [16]. Figure 1 shows the effect of mitochondrial energization on HNE-stimulated proton leak. Proton leak kinetics were measured in rat skeletal muscle mitochondria energized with succinate in the absence (Figure 1B) or presence (Figure 1C) of 50 μM HNE. Mitochondria were incubated in medium for a total of 10 min (Figure 1A) and treated with HNE for 9 min (where appropriate). Succinate (4 mM) was used to energize the mitochondria at 0.75, 2.5 or 5 min before the measurement of leak kinetics. Figure 1(B) indicates that, in the absence of HNE, rat skeletal muscle mitochondria showed an energization-dependent endogenous proton leak. Figure 1(C) shows that HNE amplified this energization-dependent proton leak.

To compare proton leak rates at the same driving force, Figure 1(D) shows rates interpolated at 166 mV, the highest membrane potential common to all curves generated in the experiment. The increase in endogenous proton leak between 0.75 and 5 min was not significant at 166 mV (although it was significant at 178 mV). Thus, measured at a driving force of 166 mV, the endogenous proton conductance does not contribute significantly to energization-dependent proton leak. However, addition of 50 μM HNE not only gave a significantly higher proton leak rate at 2.5 and 5 min when compared with the control, but also increased significantly as time of energization with succinate increased. The total time in the medium was 10 min before the measurement of each curve, therefore Figure 1 shows that HNE-stimulated proton conductance increased as the time of energization increased and not with total incubation time.

Effect of membrane potential on HNE-stimulated proton leak in rat skeletal muscle mitochondria

Previous work has demonstrated that both malonate and KCN were able to blunt energization-dependent endogenous activation of proton leak [16]. To test the ability of malonate or KCN to blunt energization-dependent HNE-stimulated proton leak, a submaximal concentration of either malonate (Figures 2A–2C) or KCN (Figures 2D and 2E) was added to rat skeletal muscle mitochondria immediately before succinate addition.

Proton leak kinetics were measured in the absence (Figure 2A) or presence (Figure 2B) of 430 μM malonate. The HNE-stimulated increase in respiration (Figure 2A minus Figure 2B) was calculated at the highest common potential, 164 mV.

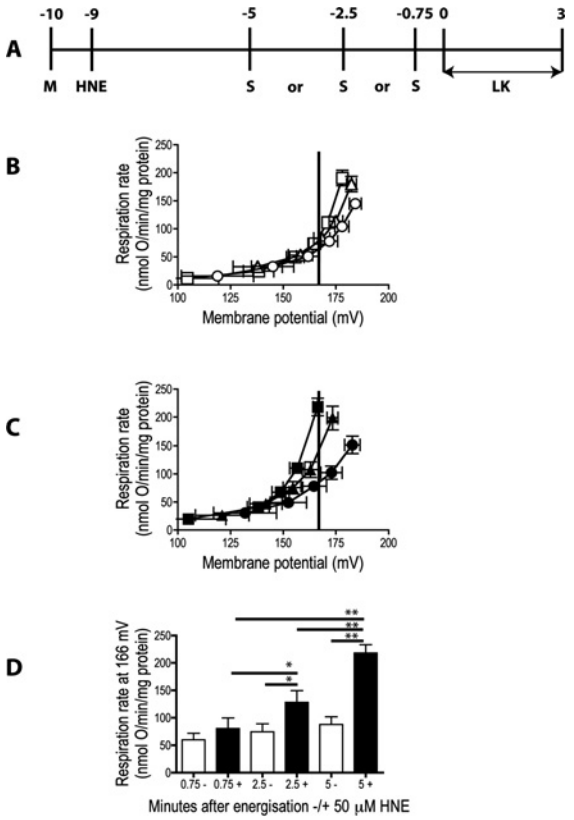

Figure 1 Energization-dependent stimulation of proton leak in rat skeletal muscle mitochondria by 50 μM HNE

Proton leak kinetics were measured in rat skeletal muscle mitochondria as described in the Experimental section. (A) Timings of additions to the incubation chamber. Mitochondria plus inhibitors (M) were added at $t = -10$ min, 50 μM HNE (where present) was added at $t = -9$ min, 4 mM succinate (S) was added at the times indicated, then leak kinetics (LK) were measured between $t = 0$ and $t = 3$ min by titration of membrane potential and oxygen consumption rate with malonate from 0.14 to 2.3 mM. The kinetic response of mitochondrial proton leak rate (measured as oxygen consumption rate) to membrane potential measured after energization with 4 mM succinate for 0.75 (circles), 2.5 (triangles) or 5.0 min (squares) was measured without (B) or with (C) 50 μM HNE. (D) Proton leak rate interpolated at 166 mV [continuous vertical lines in (B) and (C)]; the average highest protonmotive force common to all curves generated in the experiment. The results are the means ± S.E.M. of duplicate experiments performed with five separate preparations. One-way ANOVA was performed for (D); $P = 0.0001$, with Tukey's multiple comparison test used post-hoc; significant differences, $*P < 0.05$, $**P < 0.001$.

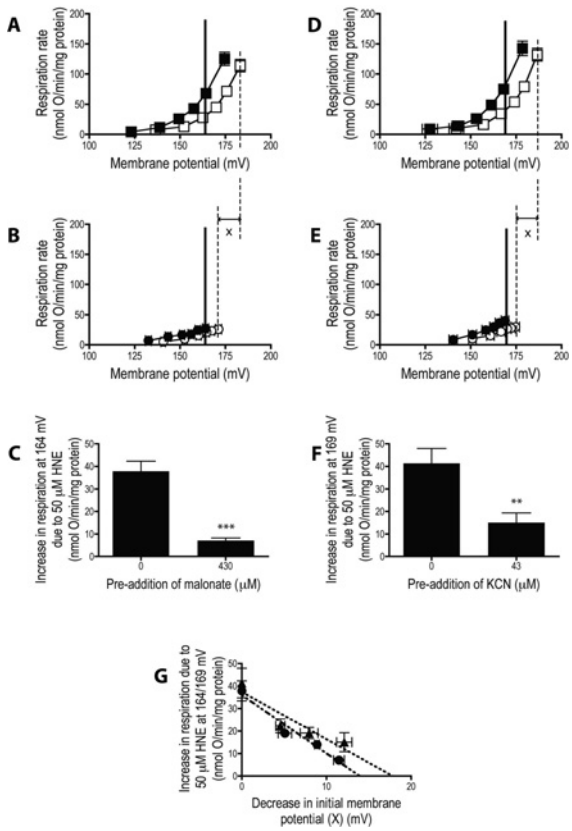

Figure 2 Sensitivity of HNE-stimulated proton leak in rat skeletal muscle mitochondria to membrane potential

(A–C) Effect of malonate, (D–F) effect of KCN and (A, B, D, E) proton leak kinetics. Succinate (4 mM) was added at $t = -1.5$ min (see Figure 1A) in the absence (open symbols) or presence (closed symbols) of 50 μM HNE. Proton leak kinetics were measured between $t = 0$ and $t = 3$ min after no treatment (A, D) or the addition of 430 μM malonate (B) or 43 μM KCN (E) immediately prior to addition of succinate. (C, F) Inhibition of HNE-stimulated proton leak by malonate and KCN. The increase in proton conductance at $t = 0$ caused by addition of 50 μM HNE was interpolated (continuous vertical lines in A, B, D, E) at the highest common membrane potential, 164 mV in (C) and 169 mV in (F). 'X' indicates the drop in membrane potential measured at $t = 0$ caused by pre-addition of malonate or KCN. (G) Effect of this drop in membrane potential on HNE-stimulated proton conductance. The increases in proton leak rate (C and results not shown) using 140 μM and 290 μM malonate (circles), and using or 14 μM and 29 μM KCN (triangles) (F and results not shown) are plotted against the decrease ('X') in membrane potential at $t = 0$ in the absence of HNE. The results are the means ± S.E.M. for five (A–C) or six (D–F) experiments each performed in duplicate. Significantly different from zero addition by paired Student's t test: $**P < 0.01$, $***P < 0.001$. Lines in (G) are linear regressions.

Figure 2(C) shows that pre-addition of 430 μM malonate led to a highly significant attenuation of HNE-stimulated proton leak.

Pre-addition of malonate could be inhibiting HNE-stimulated proton leak by lowering the protonmotive force, by altering the redox state of some component of the electron transport chain or by some direct effect of malonate itself. To rule out the latter two possibilities, the experiment in Figure 2(C) was repeated using the complex IV inhibitor, KCN, at a concentration that lowers the membrane potential to the same extent as 430 μM malonate. Proton leak kinetics were measured in the absence (Figure 2D) or presence (Figure 2E) of 43 μM KCN. The HNE-stimulated increase in respiration (Figure 2D minus Figure 2E) was calculated at the highest common membrane potential, 169 mV (Figure 2F). In the presence of 43 μM KCN, HNE-stimulated proton leak was significantly lower than in its absence. The addition of malonate limits substrate oxidation, lowers membrane potential and oxidizes electron transport chain intermediates, whereas addition of KCN reduces intermediates. Despite creating opposing redox effects, each inhibitor decreased HNE-stimulated proton leak,

suggesting that a high membrane potential is necessary for HNE action.

HNE-stimulated proton leak was also measured at intermediate concentrations of pre-added malonate or KCN (leak kinetic results not shown). This produced intermediate decreases in control membrane potential (equivalent to 'X' in Figures 2B and 2E). To characterize the ability of decreased membrane potential to blunt HNE-stimulated proton leak, Figure 2(G) shows the HNE-stimulated leak rate (e.g. Figures 2C and 2F) plotted against the drop (X) in membrane potential due to various concentrations of pre-added malonate or KCN. The linear regressions for malonate and KCN are similar, suggesting a conserved mechanism of inhibition of HNE action through the lowering of membrane potential. Extrapolation to zero effect suggests that a decrease in the state 4 membrane potential of 10–20 mV is sufficient to prevent activation of proton leak by HNE (state 4 indicates mitochondria with respiratory substrate, but no ADP or exogenous uncoupler present).

These results show that HNE-stimulated proton leak requires a high membrane potential. If membrane potential decreases by 10–20 mV, activation is prevented.

Contribution of UCP3 to HNE-stimulated proton leak assessed using skeletal muscle mitochondria from WT and *Ucp3*-KO mice

The two main candidates for activation of uncoupling of skeletal muscle mitochondria by HNE are UCP3 and ANT. The contribution of UCP3 to HNE-stimulated proton conductance after 2.5 min energization was assessed. Proton leak kinetics were measured in the presence or absence of 50 μM HNE using skeletal muscle mitochondria prepared, in parallel, from WT (Figure 3A) and *Ucp3*-KO (Figure 3B) sibling-paired mice. Figure 3(A) shows that skeletal muscle mitochondria from WT mice have a similar HNE-stimulated activation of proton leak to mitochondria from rat (Figures 1B and 1C). Figure 3(B) shows an HNE-stimulated increase in proton leak in skeletal muscle mitochondria from *Ucp3*-KO that is smaller than in WT.

The absolute contribution to proton leak by UCP3 (Figure 3A minus Figure 3B) is shown in Figure 3(C) by interpolation at the highest membrane potential common to all curves, 160 mV. UCP3-associated proton conductance is seen in the absence of HNE (as expected [16]), but is significantly higher in the presence of 50 μM HNE, showing that HNE activates proton conductance through UCP3 under these conditions. At a membrane potential of 160 mV, 50 μM HNE increased the respiration rate by 76 nmol of O/min per mg of protein in mitochondria from WT mice, and 68 nmol of O/min per mg of protein in mitochondria from *Ucp3*-KO mice; therefore approx. 11 % of HNE-stimulated proton conductance after 2.5 min energization with succinate is dependent on the presence of UCP3.

Contribution of ANT to HNE-stimulated proton leak assessed using skeletal muscle mitochondria from *Ucp3*-KO mice

To quantify the contribution of ANT to HNE-stimulated proton leak after 2.5 min energization, carboxyatractylate (a specific inhibitor of ANT) was used in skeletal muscle mitochondria isolated from *Ucp3*-KO mice to avoid potential inhibition of UCP3 by carboxyatractylate. Proton leak kinetics were measured in mitochondria lacking UCP3 in the absence (Figure 4A) or presence (Figure 4B) of 7 nmol of carboxyatractylate/mg of protein, an amount sufficient to fully inhibit ADP transport by ANT. Mitochondria were incubated in the presence of 50 μM HNE (where appropriate) and interpolation at 157 mV was used to assess the contribution of ANT (Figure 4A minus Figure 4B). Figure 4(C) shows that ANT-associated proton conductance occurred in the absence of HNE, but was significantly higher in the presence of 50 μM HNE.

For this subset of experiments and at a membrane potential 157 mV, 50 μM HNE increased respiration rates by 75 nmol of O/min per mg of protein in the absence of carboxyatractylate and 21 nmol of O/min per mg of protein in mitochondria in the presence of carboxyatractylate, therefore approx. 72 % of

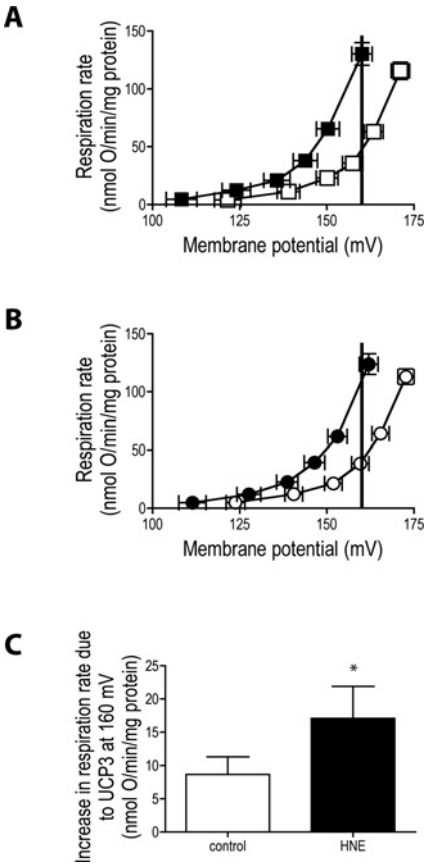

Figure 3 Contribution of UCP3 to HNE-stimulated proton leak after 2.5 min energization in mouse skeletal muscle mitochondria

Proton leak kinetics in mitochondria from wild-type (A) and *Ucp3*-KO (B) mice. Succinate (4 mM) was added at $t = -2.5$ min, without (open symbols) or with (closed symbols) 50 μM HNE. (C) Proton leak due to UCP3 measured by interpolation at 160 mV (continuous vertical lines in A, B) as (A) minus (B). The results are the means ± S.E.M. for 12 experiments, each performed in duplicate. *Significantly different from control (paired Student's *t* test; $P < 0.05$).

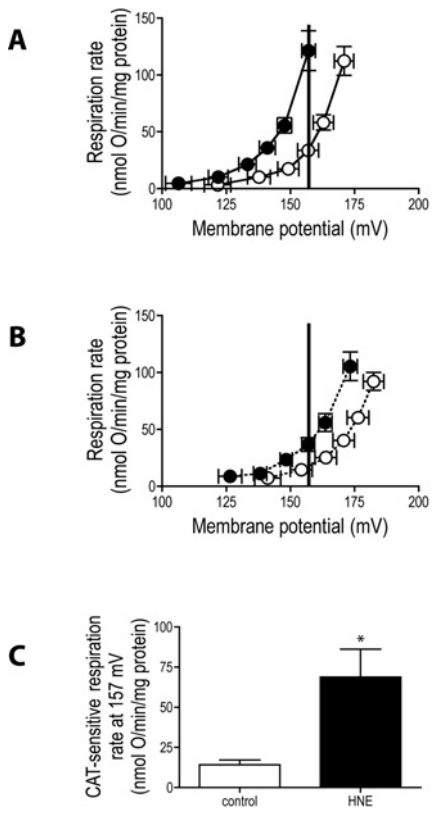

Figure 4 Contribution of ANT to HNE-stimulated proton leak after 2.5 min energization in *Ucp3*-KO mouse skeletal muscle mitochondria

(A, B) Proton leak kinetics in mitochondria from *Ucp3*-KO mice. Succinate (4 mM) was added at $t = -5$ min, without (open symbols) or with (closed symbols) 50 μM HNE in the absence (A) or presence (B) of 7 nmol of carboxyatractylate/mg of protein. (C) Proton leak due to ANT measured by interpolation at 157 mV (continuous vertical lines in A, B) as (A) minus (B). The results are the means ± S.E.M. for 6 experiments, each performed in duplicate. *Significantly different from control (paired Student's *t* test; $P < 0.03$). CAT, carboxyatractylate.

HNE-stimulated proton leak was due to ANT in mitochondria from *Ucp3*-KO mice. This implies that ANT contributes approx. 64 % of the HNE-stimulated proton conductance in skeletal muscle mitochondria from WT mice. Thus approx. 25 % of the proton conductance caused by HNE in skeletal muscle mitochondria from WT mice is through pathways other than UCP3 and ANT.

DISCUSSION

We have described a stimulation of proton conductance by HNE that increases with time after the energization of mitochondria with succinate. We have shown that energization is required to provide a high membrane potential (rather than to provide reduced intermediates of the electron transport chain) to allow HNE to increase proton conductance via UCP3, ANT and other uncoupling pathways. The effect of membrane potential may be to sensitize target proteins to HNE directly, for example, through a conformational change. Alternatively, high membrane potential may be required for the release of a secondary cofactor (such as ROS or fatty acids), or release of an activating breakdown product of HNE itself [17].

HNE was found to affect proton conductance through the activation of two known uncoupling proteins, UCP3 and ANT, confirming a previous study [7]. In the present study using mouse skeletal muscle mitochondria, the estimated relative contributions of UCP3, ANT and other pathways to HNE-stimulated proton conductance were observed to be approx. 11 %, 64 % and 25 % respectively. This is in contrast to the previous study [7], in which UCP3 and ANT were found to be the only contributors to HNE-stimulated leak, each contributing approx. 50 % of the effect (although there were complicating issues relating to non-additivity of the effects of inhibitors, subsequently resolved in [16]). This discrepancy may highlight the condition-dependence of the interaction of HNE with uncoupling pathways and may be caused by differences in energization regimes between the present work and previous study [7]. Such variations may also explain differences in activation of UCP1 by HNE observed in other laboratories [10,11]. The discrepancy may also reflect possible differences in the requirements for high membrane potential on activation of UCP3 and ANT by HNE; further work is needed to resolve this point. The observation that UCP3 catalyses approx. 11 % of the effect of HNE, whereas ANT catalyses approx. 64 %, although UCP3 is present at approx. 4 pmol/mg of protein [18] when ANT is present at approx. 2 nmol/mg of protein [19], suggests that the HNE-activated proton conductance of UCP3 is approx. 100-fold higher than that of ANT, providing a rationale for an important role of UCP3 in regulating proton conductance and ROS production, although ANT is also activatable and present in excess.

The present study has explored the conditions under which HNE stimulates the uncoupling of skeletal muscle mitochondria. Firstly, we find that length of incubation time during energization is important. Secondly, we find that a high membrane potential must be achieved during this energization. Physiologically, uncoupling by HNE is thought to be involved in the negative feedback control of mitochondrial ROS production [7], which is strongly attenuated if protonmotive force decreases [3,4]. We propose that the requirement for a high membrane potential for stimulation of proton conductance by HNE ensures that this feedback uncoupling only occurs at very high membrane potential, and prevents the uncoupling of mitochondria by non-mitochondrial ROS and its peroxidation products produced during high workload when mitochondria are functioning at a lower membrane potential.

ACKNOWLEDGEMENTS

We thank Dr Mary-Ellen Harper (Department of Biochemistry, Microbiology and Immunology, Faculty of Medicine, University

of Ottawa, Ottawa, Canada) for *Ucp3*-KO mice, and Julie Buckingham and Helen Boysen for technical assistance. This work was supported by the Medical Research Council and the Wellcome Trust (grants 065326/Z/01/Z and 066750/B/01/Z).

REFERENCES

1 Halliwell, B. and Gutteridge, J. M. C. (1999) Free Radicals in Biology and Medicine. 3rd edn, Oxford University Press, New York
2 Brand, M. D., Buckingham, J. A., Esteves, T. C., Green, K., Lambert, A. J., Miwa, S., Murphy, M. P., Pakay, J. L., Talbot, D. A. and Echtay, K. S. (2004) Mitochondrial superoxide and aging: uncoupling-protein activity and superoxide production. Biochem. Soc. Symp. 71, 203–213
3 Miwa, S. and Brand, M. D. (2003) Mitochondrial matrix reactive oxygen species production is very sensitive to mild uncoupling. Biochem. Soc. Trans. 31, 1300–1301
4 Papa, S. and Skulachev, V. P. (1997) Reactive oxygen species, mitochondria, apoptosis and aging. Mol. Cell. Biochem. 174, 305–319
5 Brand, M. D. (2000) Uncoupling to survive? The role of mitochondrial inefficiency in ageing. Exp. Gerontol. 35, 811–820
6 Esterbauer, H., Schaur, R. J. and Zollner, H. (1991) Chemistry and biochemistry of 4-hydroxynonenal, malonaldehyde and related aldehydes. Free Radical Biol. Med. 11, 81–128
7 Echtay, K. S., Esteves, T. C., Pakay, J. L., Jekabsons, M. B., Lambert, A. J., Portero-Otin, M., Pamplona, R., Vidal-Puig, A. J., Wang, S., Roebuck, S. J. and Brand, M. D. (2003) A signalling role for 4-hydroxy-2-nonenal in regulation of mitochondrial uncoupling. EMBO J. 22, 4103–4110
8 Cannon, B., Shabalina, I. G., Kramarova, T. V., Petrovic, N. and Nedergaard, J. (2006) Uncoupling proteins: a role in protection against reactive oxygen species – or not? Biochim. Biophys. Acta 1757, 449–458
9 Echtay, K. S., Pakay, J. L., Esteves, T. C. and Brand, M. D. (2005) Hydroxynonenal and uncoupling proteins: a model for protection against oxidative damage. Biofactors 24, 119–130
10 Esteves, T. C., Parker, N. and Brand, M. D. (2006) Synergy of fatty acid and reactive alkenal activation of proton conductance through uncoupling protein 1 in mitochondria. Biochem. J. 395, 619–628
11 Shabalina, I. G., Petrovic, N., Kramarova, T. V., Hoeks, J., Cannon, B. and Nedergaard, J. (2006) UCP1 and defense against oxidative stress. 4-Hydroxy-2-nonenal effects on brown fat mitochondria are uncoupling protein 1-independent. J. Biol. Chem. 281, 13882–13893
12 Gong, D. W., Monemdjou, S., Gavrilova, O., Leon, L. R., Marcus-Samuels, B., Chou, C. J., Everett, C., Kozak, L. P., Li, C., Deng, C. et al. (2000) Lack of obesity and normal response to fasting and thyroid hormone in mice lacking uncoupling protein-3. J. Biol. Chem. 275, 16251–16257
13 Cadenas, S., Echtay, K. S., Harper, J. A., Jekabsons, M. B., Buckingham, J. A., Grau, E., Abuin, A., Chapman, H., Clapham, J. C. and Brand, M. D. (2002) The basal proton conductance of skeletal muscle mitochondria from transgenic mice overexpressing or lacking uncoupling protein-3. J. Biol. Chem. 277, 2773–2778
14 Rolfe, D. F. S., Hulbert, A. J. and Brand, M. D. (1994) Characteristics of mitochondrial proton leak and control of oxidative phosphorylation in the major oxygen-consuming tissues of the rat. Biochim. Biophys. Acta 1188, 405–416
15 Brand, M. D. (1995) Measurement of mitochondrial protonmotive force. Bioenergetics – A Practical Approach (Brown, G. C. and Cooper, C. E., eds), pp. 39–62, IRL Press, Oxford
16 Parker, N., Affourtit, C., Vidal-Puig, A. J. and Brand, M. D. (2008) Energisation-dependent endogenous activation of proton conductance in skeletal muscle mitochondria, Biochem. J. 412, 131–139
17 Ullrich, O., Grune, T., Henke, W., Esterbauer, H. and Siems, W. G. (1994) Identification of metabolic pathways of the lipid peroxidation product 4-hydroxynonenal by mitochondria isolated from rat kidney cortex. FEBS Lett. 352, 84–86
18 Harper, J. A., Stuart, J. A., Jekabsons, M. B., Roussel, D., Brindle, K. M., Dickinson, K., Jones, R. B. and Brand, M. D. (2002) Artifactual uncoupling by uncoupling protein 3 in yeast mitochondria at the concentrations found in mouse and rat skeletal-muscle mitochondria. Biochem. J. 361, 49–56
19 Brand, M. D., Pakay, J. L., Ocloo, A., Kokoszka, J., Wallace, D. C., Brookes, P. S. and Cornwall, E. J. (2005) The basal proton conductance of mitochondria depends on adenine nucleotide translocase content. Biochem. J. 392, 353–362

Received 11 January 2008/12 March 2008; accepted 2 April 2008
Published as Immediate Publication 2 April 2008, doi 10.1042/BSR20080002